J Therm Anal Calorim (2011) 103:59–64
DOI 10.1007/s10973-010-1137-6

Thermoanalytical studies of imidazole-substituted coordination compounds

Mn(II)-complexes of bis(1-methylimidazol-2-yl)ketone

S. Materazzi · S. Vecchio · L. W. Wo · S. De Angelis Curtis

AICAT2010 Special Chapter

Abstract Four manganese(II) coordination compounds with bis(1-methylimidazol-2-yl)ketone (BIK) of general formula $Mn(BIK)_2X_2$ (X = Cl, Br, NO_3, ClO_4) were synthesized and characterized by elemental analysis, by UV–vis, and FTIR spectroscopies to be compared with the literature data. Following our previous thermoanalytical studies on imidazole-substituted coordination compounds, the thermal behavior of the synthesized Mn(II) complexes was investigated using TG and DTG techniques: the thermal profile is characterized by three substantial consecutive releasing steps for all the three complexes and the releasing supposed behavior is confirmed by EGA analysis performed by coupling the TG analyzer to an MS spectrometer. In particular, the first step is ascribed to the release of the two anions, followed by the loss of four methyl groups (side chains of the ligand) and two bridge-carbonyl groups. The residual tetra-imidazole manganese compound decomposes in a final step to give MnO as the final residue. Both the initial decomposition temperatures and the kinetic rate constants associated to the first decomposition step indicated a higher stability of the $Mn(BIK)_2Cl_2$ complex, the bromide complex being very close to the chloride one (first-step thermal stability: $ClO_4^- < NO_3^- \leq Br^- < Cl^-$). Finally, the three-dimensional diffusion reaction model (D3) was selected to describe the first decomposition step for all the four complexes examined.

Keywords Manganese(II) coordination compounds · Bis(1-methylimidazol-2-yl)ketone · TG · DTG · UV–vis · MS · Evolved gas analysis · Thermal stability · TG–MS

S. Materazzi (✉) · S. De Angelis Curtis
Department of Chemistry, Sapienza University of Rome, P.le A. Moro, 5, 00185 Rome, Italy
e-mail: stefano.materazzi@uniroma1.it

S. Vecchio
Department S.B.A.I, Sapienza University of Rome, Via del Castro Laurenziano 7, 00161 Rome, Italy

L. W. Wo
Department of Chemistry, Illinois State University, Normal, IL, USA

Introduction

Manganese(II) coordination compounds with nitrogen donor ligands like substituted imidazoles have been thoroughly investigated during the past years. These compounds can be good models to simulate several industrial applications like the behavior of manganese compounds containing enzymes as catalysts for the polymerization of olefins [1–12] and for washing and bleaching purposes. The improvement of classical washing and bleaching processes is both economically and ecologically relevant. The use of catalytically active transition metal complexes, which can activate hydrogen peroxide, might be a means of achieving these aims.

Several manganese complexes with polydentate N-donor ligands have been patented for this purpose [1–3]. Manganese complexes are also important as model compounds for manganese-containing enzymes such as superoxide dismutase, catalases, or extradiol-cleaving catechol dioxygenases. In catalases and extradiol-cleaving catechol dioxygenases, the manganese ion is usually coordinated by histidine and aspartate or glutamate residues. In order to mimic the histidines, many model complexes comprise bi- or tridentate N-donor ligands such as 2,2′-bipyridine, hydrotris(pyrazol-1-yl)borate, or triazacyclononane [4–7]. Manganese(II) complexes containing N-donor ligands have

also been tested as polymerization catalysts for olefins, especially ethene. The hitherto published results are promising, though still far from those of established catalyst systems [8–12].

In this view, thermoanalytical characterizations are useful to complete the information related to the metal-binding sites and to relate their physico-chemical properties. In addition, the Evolved Gas Analysis allows confirming the proposed decomposition steps. Several articles have been published by our group in this field [13–21]. A thermoanalytical study of bis(imidazol-2-yl)methane (BIM) complexes with cobalt, copper, and nickel has already been reported by our group, since BIM is the simplest polyimidazole ligand useful to model multihistidine coordination [17].

Bis(1-methylimidazol-2-yl)ketone (BIK) (Fig. 1) has been known to be a versatile *N,N* ligand for many transition metals since its first synthesis in 1977 [22].

In this study, following the experimental conditions reported in the literature [23], the synthesis and the thermoanalytical study of bis(1-methylimidazl-2yl)ketone(BIK) complexes with divalent manganese having a general formula $Mn(BIK)_2X_2$ are reported (X = Cl, Br, NO_3, or ClO_4). The thermal stability and the decomposition steps were determined by thermogravimetry (TG) and derivative thermogravimetry (DTG). The released products, due to the thermal decomposition, were analyzed by online coupling mass spectrometer to the thermobalance; the so obtained evolved gas analysis (EGA–MS) allowed to prove the proposed decomposition steps.

Experimental and methods

Materials

For all the complexes of general formula $Mn(BIK)_2X_2$, a 20 mL methanol solution of 900 mg of BIK (about 4.8 mmol) was added to 2.4 mmol methanol solutions of, respectively $MnCl_2$, $MnBr_2$, $Mn(NO_3)_2$, or $Mn(ClO_4)_2$. After few minutes of warm stirring, the solvent was gently removed to precipitate the complexes. A similar procedure has also been reported in the literature [23]. The reaction is shown in the Scheme 1.

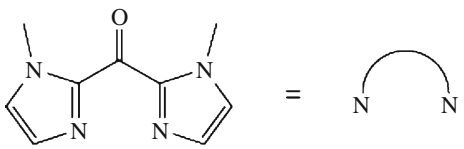

Fig. 1 The ligand bis(1-methylimidazol-2-yl)ketone (BIK)

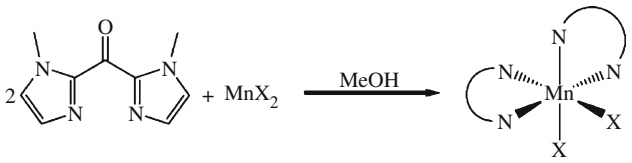

Scheme 1 Synthesis of the complexes. X = Cl, Br, NO_3, or ClO_4

Instrumental

Elemental analysis was performed by a VarioEl III CHN Analyzer; UV–vis by a Perkin Elmer Lambda Series, and FTIR measurements by a Perkin Elmer 1760X instrument. TG curves were recorded using a Perkin Elmer TGA7 equipment. The samples investigated of approximately 7–8 mg were heated in platinum crucibles in the temperature range between 20 and 850 °C, under an atmosphere of pure nitrogen or air (gaseous mixture of nitrogen and oxygen with 80 and 20%, v/v, respectively) under a flow rate of 100 mL min^{-1}. The thermal behavior was investigated using TG data at 10 K min^{-1} because of its best resolution.

Mass spectra of the gases evolved during the experiments were recorded by a simultaneous TG/DTA apparatus (STD 2960 simultaneous DTA–TGA, TA Instruments Inc., USA) using sealed crucibles with a pinhole on the top. The gaseous species were analyzed by a ThermoStar GDS 200 (Balzers Instrument) quadrupole mass spectrometer equipped with Chaneltron detector, through a heated 100% methyl deactivated fused silica capillary tubing. Data collection was carried out with QuadStar 422v60 software in multiple ion detection mode (MID).

Kinetic methods

The kinetic parameters of decomposition processes were determined from TG experiments carried out at several heating rates (β) between 2.5 and 20 K min^{-1}, using the isoconversional Ozawa–Flynn–Wall (OFW) [24, 25], according to the following equation:

$$\ln \beta = \ln\left(\frac{A_\alpha R}{E_\alpha}\right) - \ln g(\alpha) - 5.3305 - 1.052\left(\frac{E_\alpha}{R}\right)\left(\frac{1}{T_\alpha}\right) \quad (1)$$

where E_α and A_α are the activation energy and the pre-exponential factor at a given degree of conversion α, respectively. Once the Doyle's approximation [26]: $\ln p(x) \approx -5.3305 - 1.052x$, where $x = E_\alpha/(RT_\alpha)$ and $20 \leq x \leq 60$) is verified to be valid over the entire range of α, then, from the slopes of the related regression straight lines derived by the $\ln(\beta)$ versus $1/T_\alpha$ plots, the corresponding E_α values are derived at any selected value of α.

Model-fitting kinetic methods are usually considered to be unable to show the variation of the activation energy with

the extent of reaction that is usually observed in thermal decomposition processes that show a multistep nature [27]. Moreover, one of these methods (namely, the Coats–Redfern (CR) method [28]) can be used to obtain 14 single pairs of Arrhenius parameters values (E and A), one for each of the 14 integral $g(\alpha)$ model functions, representing the most commonly cited in the literature [26, 28]. It is possible to estimate the isoconversional pre-exponential factor ($\ln A_{\alpha}$) if the values of the Arrhenius parameters determined by the CR method for the 14 model functions are linearly dependent, according to the following compensation behavior:

$$\ln A_j = a + bE_j \quad (2)$$

where the subscript j is related to each integral $g(\alpha)$ model function. Once the intercept (a) and the slope (b) have been determined from Eq. 2, the isoconversional pre-exponential factor is calculated at each fixed degree of conversion α using the isoconversional activation energy values derived by Eq. 1. Once the isoconversional values of $\ln A_{\alpha}$ and E_{α} are determined, the integrated model function $g(\alpha)$ can be numerically reconstructed using a procedure reported in detail in the literature [26, 28]. The best model function is selected by evaluating which $g(\alpha)$ function (among the 14 models considered) has its conversion-dependent mathematical expression that best fits the values of the integral $g(\alpha)$ model function determined by the numerical reconstruction over the entire range of α values.

Finally, because of the occurrence of a compensation effect, neither activation energy nor pre-exponential factor could be considered as a stability parameter. In this case, the most reasonable parameter could be the isoconversional rate constant (k_{α}), calculated at a mean temperature $\langle T \rangle$ (over the experimental temperature range for all the complexes investigated) using the isoconversional values of $\ln A_{\alpha}$ and E_{α} according to the Arrhenius equation.

Results and discussion

Elemental analysis data of the complexes considered in this study were summarized in Table 1. As a result of the good agreement between experimental and calculated data a general formula $Mn(BIK)_2X_2$ (where X = Cl, Br, NO_3, ClO_4) can be hypothesized. The $Mn(BIK)_2Cl_2$ complex was also characterized by UV–vis and FTIR spectroscopies to be compared with the corresponding literature data.

The manganese complexes showed IR bands (KBr) at 1630 cm^{-1} (m, C=O), 1480 cm^{-1} (w), 1463 cm^{-1} (w), 1415 cm^{-1} (s, C=N), 1290 cm^{-1} (w), and 1170 cm^{-1} (w). The UV–vis spectrum in acetonitrile showed a λ_{max} (log e) = 325 (4.51) nm. The ligand BIK absorbs ultraviolet light at 318 nm (log e = 4.22). This strong absorption results almost exclusively from an electron transition from the HOMO − 1 into the LUMO.

Looking at the thermal behavior, with respect to the BIM complexes, where only one main thermal decomposition step is present [17] in the TG curves of all the complexes tested in this study (under a dynamic air flow), the BIK complexes are characterized by a first releasing step of the anions, followed by the loss of four methyl groups (side chains) and two bridge-carbonyl groups. The residual tetra-imidazole manganese compound decomposes in a final step to give the metal oxide as the final residue.

The TG curve of the $Mn(BIK)_2Cl_2$ is reported in Fig. 2 as an example and evidences the described three steps occurring in the temperature ranges 20–220, 220–360, and 360–580 °C, respectively.

Table 2 reports the calculated and the found mass loss for each complex. The experimental and the calculated results are in good agreement.

The scheme summarizes the proposed TG releasing steps (X = Cl, Br, NO_3, and ClO_4):

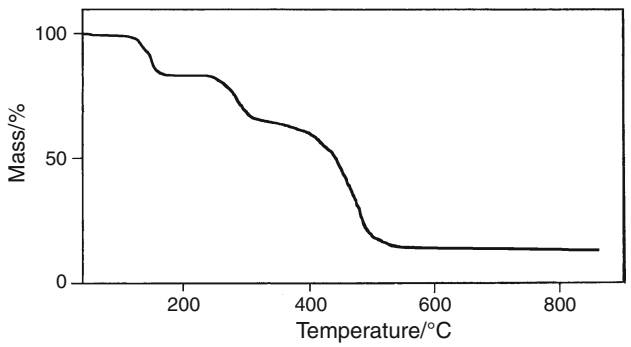

Fig. 2 TG curve of $Mn(BIK)_2Cl_2$ at a heating rate of 10 K min^{-1} (100 mL min^{-1} air flow)

Table 1 Results of elemental analysis

Complex	C/%		H/%		N/%		Mn/%	
	Found	Calculated	Found	Calculated	Found	Calculated	Found	Calculated
$Mn(BIK)Cl_2$	42.7	42.7	4.1	4.0	22.3	22.3	10.8	10.8
$Mn(BIK)Br_2$	36.2	36.3	3.3	3.4	18.8	18.8	9.2	9.2
$Mn(BIK)(NO_3)_2$	38.7	38.6	3.5	3.6	25.1	25.0	9.8	9.8
$Mn(BIK)(ClO_4)_2$	40.5	40.4	3.8	3.7	21.0	20.9	10.2	10.2

The manganese has been determined by ICP–OES

Table 2 Experimental mass loss percentages determined by TG and comparison with calculated ones, obtained by taking into account the proposed reaction mechanisms

Compound	Exper loss 1st TG step (calculated)	Exper loss 2nd TG step (calculated)	Res after 3rd TG step (calculated)
$Mn(BIK)_2Cl_2$	−13.5%	−23.2	13.8%
	($-2Cl = -13.9\%$)	($-C_6H_{12}O_2 = -23.0\%$)	(Res MnO = 14.0%)
$Mn(BIK)_2Br_2$	−26.8%	−20.0%	12.3%
	($-2Br = -26.9\%$)	($-C_6H_{12}O_2 = -19.5\%$)	(Res MnO = 11.9%)
$Mn(BIK)_2(NO_3)_2$	−22.0	−20.5	12.6%
	($-2NO_3 = -22.2\%$)	($-C_6H_{12}O_2 = -20.7\%$)	(Res MnO = 12.7%)
$Mn(BIK)_2(ClO_4)_2$	−31.6%	−16.8%	11.3%
	($-2ClO_4 = -31.4\%$)	($-C_6H_{12}O_2 = -18.3\%$)	(Res MnO = 11.2%)

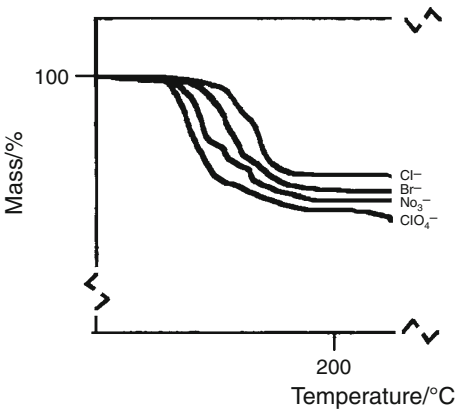

Fig. 3 TG curves of the first step of mass loss for all the complexes investigated at a heating rate of 10 K min^{-1} (100 mL min^{-1} air flow)

$$Mn(BIK)_2X_2 \xrightarrow{-2X} Mn(BIK)_2 \xrightarrow{-2CO-4Met} Mn(Im)_4 \xrightarrow{-4Imid} MnO$$

By zooming in the first part of all the thermogravimetric profiles (temperature range 20–220 °C), the TG curves related to the first decomposition step of the four complexes are collected and compared in Fig. 3. The stability scale constructed on the basis of the initial (onset) temperatures related to the first decomposition step only (Fig. 3) indicates a higher stability of the $Mn(BIK)_2Cl_2$ complex structure, followed by the bromide and nitrate complexes, with the thermal stability of the bromide complex closer to that of the chloride one (first-step thermal stability scale: $ClO_4^- < NO_3^- < Br^- < Cl^-$).

The EGA analysis performed by coupling the TG analyzer to an MS spectrometer allowed confirming the

Table 3 Arrhenius parameters related to the first decomposition step of $Mn(BIK)Cl_2$ at 10 K min^{-1} obtained by the Coats–Redfern method for the most commonly used model functions

N	Model function	$g(\alpha) = k \cdot t$	*E*/kJ mol^{-1}	$\ln(A/min^{-1})$	R^2
1	Power law	$(\alpha)^{1/4}$	21.3	1.9	0.9969[a]
2	Power law	$(\alpha)^{1/3}$	32.9	4.6	0.9975[a]
3	Power law	$(\alpha)^{1/2}$	55.9	10.5	0.9971[a]
4	Power law	$(\alpha)^{3/2}$	193.9	45.5	0.9985[a]
5	One-dimensional diffusion	$(\alpha)^2$	262.8	62.5	0.9982[a]
6	Mampel (first-order)	$-\ln(1-\alpha)$	160.6	38.2	0.9905
7	Avrami-Erofeev	$[-\ln(1-\alpha)]^{1/4}$	30.3	4.2	0.9821
8	Avrami-Erofeev	$[-\ln(1-\alpha)]^{1/3}$	44.8	7.9	0.9878
9	Avrami-Erofeev	$[-\ln(1-\alpha)]^{1/2}$	73.7	15.7	0.9871
10	Three-dimensional diffusion	$[1-(1-\alpha)^{1/3}]^2$	78.8	16.6	0.9983[a]
11	Contracting sphere	$1-(1-\alpha)^{1/3}$	32.9	4.6	0.9976[a]
12	Contracting cylinder	$1-(1-\alpha)^{1/2}$	141.5	31.8	0.9979[a]
13	Zero-order	α	124.4	28.2	0.9981[a]
14	Second-order	$(1-\alpha)^{-1} - 1$	206.7	50.9	0.9661
			$\ln(A/min^{-1}) = -(3.6 \pm 0.3) + (0.255 \pm 0.002)E$[b]		

[a] Statistically equivalent models (95% confidence level)

[b] $R^2 = 0.9989$

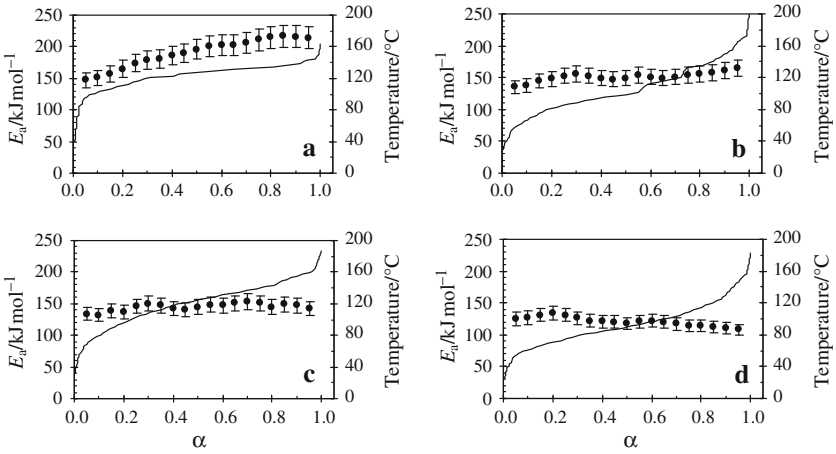

Fig. 4 Conversion dependencies of temperature (*solid line*) and activation energy (*black circles*) for all the $Mn(BIK)_2X_2$ complexes investigated. **a** $Mn(BIK)_2Cl_2$, **b** $Mn(BIK)_2Br_2$, **c** $Mn(BIK)_2(NO_3)_2$, and **d** $Mn(BIK)_2(ClO_4)_2$

proposed general decomposition mechanism. As a representative example, the nitrate complex decomposition by TG–MS coupled analysis is reported: fragments at m/z 30 (NO^+) and 44 (N_2O^+) confirmed the release of the nitrate ion, while in the temperature range 220–320 °C the fragments with m/z 44 (CO_2^+), 22 (CO_2^{2+}), 18 (H_2O^+), and 17 (OH^+) confirmed the proposed release of CO (oxidated to CO_2) and the oxidation of the methyl groups to water and carbon dioxide.

The application of the CR model-fitting kinetic method to the first decomposition step occurring in all complexes tested gave a pair of Arrhenius E and ln$A$ values for each of the 14 model functions considered (Table 3) that show to be linearly dependent according to Eq. 2. In addition, several model functions can be considered statistically equivalent, thus avoiding the selection of a suitable model function describing reasonably the decomposition mechanism, as it is commonly found in the literature and stated by Vyazovkin et al. [27]. The isoconversional OFW method enables to show in Fig. 4 the conversion dependency of both temperature and activation energy for the first decomposition step of the four complexes. Change of activation energy is negligible for complexes with Br, NO_3, and ClO_4, while a slight increasing trend is found for the Cl complex. Owing to the compensation behavior neither activation energy, nor pre-exponential factor can be considered as a stability parameter. The most reasonable parameter could be the isoconversional rate constant (k_α), calculated at a mean temperature ($\langle T \rangle = 110$ °C in this study) using the isoconversional values of E_α and lnA_α, being the latter data calculated from the former ones according to Eq. 2, where the linear fitting parameter a and b are those reported in Table 3. The k_α values (expressed in min^{-1} and calculated at 110 °C) for Cl, Br, NO_3, and ClO_4 complexes are: 1.81×10^{-6}, 3.43×10^{-6}, 4.34×10^{-6}, and 3.56×10^{-5}, respectively. On the basis of these values the following increasing order of the (kinetic) thermal stability can be assessed: $ClO_4^- < NO_3^- \leq Br^- < Cl^-$.

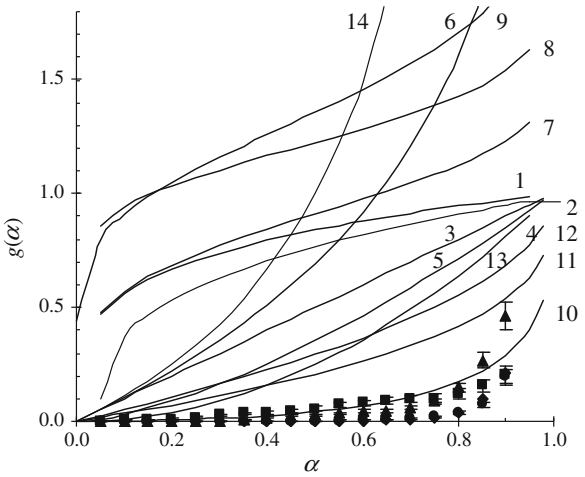

Fig. 5 Conversion dependence of $g(\alpha)$ for the 14 model functions listed in Table 3 (*thick line*) and for the experimental (reconstructed) data related to the first decomposition step. *Filled square* $Mn(BIK)_2Cl_2$, *filled diamond* $Mn(BIK)_2Br_2$, *filled triangle* $Mn(BIK)_2(NO_3)_2$, and *filled circle* $Mn(BIK)_2(ClO_4)_2$

Finally, since no significant changes of activation energy were observed in all the complexes studied with the extent of decomposition (Fig. 4), the most suitable model function was selected from the best agreement between the $g(\alpha)$ values reconstructed according to the procedure reported in the literature [26, 29] with those calculated using the expressions in Table 3 (Fig. 5). It is evident that the best fit is shown by the three-dimensional diffusion reaction model (D3), which was selected to describe the first decomposition step for all the four complexes examined.

References

1. Hage R, Lienke A. Applications of transition-metal catalysts to textile and wood-pulp bleaching. Angew Chem Int Ed. 2006;45:206–22.

2. Hage R, Lienke A. Bleach and oxidation catalysis by manganese-1,4,7-triazacylononane complexes and hydrogen peroxide. J Mol Cat A. 2006;251(1–2):150–8.
3. Reinhardt G, Jonas E, Kewitz D, Karadag A, Prehler H (Clariant), EP-B-1445305 (2004).
4. Wu AJ, Penner-Hahn JE, Pecoraro VL. Structural, spectroscopic, and reactivity models for the manganese catalases. Chem Rev. 2004;104(2):903–38.
5. Triller MU, Hsieh W-Y, Pecoraro VL, Rompel A, Krebs B. Preparation of highly efficient manganese catalase mimics. Inorg Chem. 2002;41(21):5544–54.
6. Triller MU, Pursche D, Hsieh W-Y, Pecoraro VL, Rompel A, Krebs B. Catalytic oxidation of 3,5-di-tert-butylcatechol by a series of mononuclear manganese complexes: synthesis, structure, and kinetic investigation. Inorg Chem. 2003;42(20): 6274–83.
7. Kloskowski M, Krebs B. Synthese und Charakterisierung neuer fünf- und sechsfach koordinierter Mangan(II)-Komplexe als Modellsysteme für manganabhängige Catecholdioxygenasen Z. Anorg. Allg. Chem. 2006;632:771–8.
8. Ban HT, Kase T, Murata M. Manganese-based transition metal complexes as new catalysts for olefin polymerizations. J Polym Sci A. 2001;39:3733–8.
9. Vierle M, Zhang Y, Herdtweck E, Bohnenpoll M, Nuyken O, Kühn FE. Highly reactive polyisobutenes prepared with manganese(II) complexes as initiators. Angew Chem Int Ed. 2003;42: 1307–10.
10. Nabika M, Seki Y, Miyatake T, Ishikawa Y, Okamoto K, Fujisawa K. Manganese catalysis with scorpionate ligands for olefin polymerization. Organometallics. 2004;23(19):4335–7.
11. Yliheikkilä K, Axenov K, Räisänen MT, Klinga M, Lankinen MP, Kettunen M, Leskelä M, Repo T. Manganese(II) complexes in ethene polymerization. Organometallics. 2007;26(4):980–7.
12. Nabika M, Kiuchi S, Miyatake T, Okamoto K-I, Fujisawa K. Manganese(II) halogeno complexes with neutral tris(3,5-diisopropyl-1-pyrazolyl)methane ligand: synthesis and ethylene polymerization. J Mol Cat A. 2007;269(1–2):163–8.
13. Materazzi S, Kurdziel K, Tentolini U, Bacaloni A, Aquili S. Thermal stability and decomposition mechanism of 1-allylimidazole coordination compounds: a TG-FTIR study of Co(II), Ni(II) and Cu(II) hexacoordinate complexes. Thermochim Acta. 2003;395(1–2):133–7.
14. Materazzi S, D'Ascenzo G, Aquili S, Kadish KM, Bear JL. Thermoanalytical characterization of solid-state Co(II)-, Ni(II)- and Cu(II)-4(5)-aminoimidazole-5(4)-carboxamide complexes. Thermochim Acta. 2003;397(1–2):129–34.
15. Materazzi S, Aquili S, De Angelis Curtis S, Bianchetti C, D'Ascenzo G, Kadish KM, Bear JL. The decomposition mechanism of new solid-state 4(5)-aminoimidazole-5(4)-carboxamide coordination compounds. Thermochim Acta. 2004; 409(2):145–50.
16. Materazzi S, Aquili S, De Angelis Curtis S, Vecchio S, Kurdziel K, Sagone F. Biomimetic complexes: thermal stability, kinetic study and decomposition mechanism of Co(II)-, Ni(II)- and Cu(II)-4(5)-hydroxymethyl-5(4)-methylimidazole complexes. Thermochim Acta. 2004;421:19–24.
17. Materazzi S, Aquili S, Kurdziel K, Vecchio S. Biomimetic polyimidazole complexes: a thermoanalytical study of Co(II)-, NI(II)- and Cu(II)-bis(imidazol-2-yl)methane complexes. Thermochim Acta. 2007;457:7–10.
18. De Angelis Curtis S, Kurdziel K, Materazzi S, Vecchio S. Crystal structure and thermoanalytical study of a manganese (II) complex with 1-allylimidazole. J.Therm.Anal.Calorim. 2008;92(1): 109–14.
19. Materazzi S, Gentili A, Curini R. Application of evolved gas analysis: part 1: EGA by infrared spectroscopy. Talanta. 2006; 68(3):489–96.
20. Materazzi S, Vecchio S. Evolved gas analysis by infrared spectroscopy. Appl Spectr Rev. 2010;45(4):241–73.
21. Materazzi S, Gentili A, Curini R. Application of evolved gas analysis: part 2: EGA by mass spectrometry. Talanta. 2006;69(4) :781–94.
22. Regel E, Büchel K-H. C-acylierung von 5 gliedrigen *N*-heterocyclen, I. Acylierung an C-2 von imidazolen und benzimidazolen liebigs. Ann Chem. 1977;1:145–58.
23. Peters L, Tepedino M-F, Haas T, Hübner E, Zenneck U, Burzlaff N. Syntheses and structures of mononuclear manganese(II) complexes bearing bis(1-methylimidazol-2-yl)ketone ligands. Inorg Chim Acta. 2009;362(8):2678–85.
24. Flynn JH, Wall LA. A quick direct method for the determination of activation Energy from thermogravimetric data. J Polym Sci B: Polym Lett. 1966;4(5):323–8.
25. Ozawa T. A new method of analyzing thermogravimetric data. Bull Chem Soc Jpn. 1965;38:1881–6.
26. Doyle CD. Estimating isothermal life from thermogravimetric data. J Appl Polym Sci. 1962;6(24):639–42.
27. Vyazovkin S, Wight CA. Ammonium dinitramide: kinetics and mechanism of thermal decomposition. J Phys Chem A. 1997;101: 5653–8.
28. Coats AW, Redfern JP. Kinetic parameters from thermogravimetric data. Nature. 1964;201:68–9.
29. Vecchio S, Di Rocco R, Ferragina C. Kinetic analysis of the oxidative decomposition in γ-zirconium and γ-titanium phosphate intercalation compounds. The case of 2,2′-bipyridyl and its copper complex formed in situ. Thermochim Acta. 2008;467:1–10.